*The paper was published in the proceedings of the 11th International Conference on Physical Modelling in Geotechnics (ICPMG2026) and was edited by Ioannis Anastasopoulos. The conference was held from June 8th to June 12th 2026 in Zurich, Switzerland.*

Proceedings of the 11th ICPMG 2026
11th International Conference on Physical Modelling in Geotechnics
8-12 June 2026, Zurich, Switzerland


# Evaluation of the long-term behaviour of monopile foundations under cyclic lateral loading using 1g physical modelling

M. Hajialilue-Bonab
*Professor, Department of Civil Engineering, University of Tabriz, Tabriz, Iran,* hajialilue@tabrizu.ac.ir

A. Pazhouhandeh, E. Maleki Tabrizi
*Graduate Student, Department of Civil Engineering, University of Tabriz, Tabriz, Iran,* pazhouhandehamin@gmail.com, emad.malekitabrizi@gmail.com

S. Rahnema
*Graduate Student, Department of Civil Engineering, Sharif University of Technology, Tehran, Iran,* salar.rahnema@sharif.edu

**ABSTRACT:** Monopiles are the predominant foundation type for Offshore Wind Turbines (OWTs), which experience intense cyclic lateral loading throughout their service life. However, predicting their long-term serviceability remains challenging due to limitations in existing design models that often neglect high-cycle soil–structure interaction effects. This study investigates the long-term behaviour of rigid monopiles in saturated sand using 1g physical modelling, addressing key knowledge gaps in predicting high-cycle performance. Two laboratory-scale tests, designed to replicate extended operational conditions, were subjected to 10,000 cycles of one-way lateral loading. The results consistently show that most of the accumulated lateral displacement occurs during the initial loading cycles (e.g., about 50% within the first 600 cycles), after which the accumulation rate decreases markedly and eventually approaches a stable value. Analysis of hysteresis loops revealed that the soil–pile resilient stiffness initially decreases (up to 1,500 cycles) due to sand fabric rearrangement, but later increases and stabilizes as soil densification develops under prolonged cyclic loading. Moreover, doubling the cyclic load amplitude produced more than twice the accumulated displacement, underscoring the non-linear nature of the foundation response. These findings provide valuable insights for improving Serviceability Limit State (SLS) assessments of OWT monopiles.

## 1 INTRODUCTION

The growing global demand for renewable energy has accelerated the development of offshore wind energy as a key pillar of sustainable power generation (Wojtaszek et al., 2025). Offshore wind turbines (OWTs) are increasingly being installed in deeper waters and harsher environments, where the foundation system plays a crucial role in ensuring structural integrity and long-term serviceability. Among various foundation types, monopile foundations have become the most widely adopted solution for supporting OWTs, accounting for more than 80% of current installations (Malekjafarian et al., 2021). Traditionally, monopile diameters ranged from approximately 4 to 10 m with embedded lengths of about 20 to 40 m, making them a cost-effective and structurally efficient solution for water depths up to around 40 m (Malekjafarian et al., 2021). However, with the rapid growth of offshore wind turbines, monopile diameters have increased significantly in recent years and continue to grow, enabling their application in deeper waters and for larger turbine capacities (Alsharedah 2025).

Monopile foundations are inevitably subjected to a combination of lateral, vertical, and moment loads at the pile head, primarily arising from environmental actions such as wind, waves, currents, and tidal forces (Arvan et al., 2023). Among these, lateral loads are often the most critical for design, as they govern both the ultimate and Serviceability Limit States (SLS) (Lalicata et al., 2020). The lateral response of monopiles is largely governed by the development of limiting soil resistance profiles around the pile and the depth over which these resistances are mobilized (Guo, 2006). Laboratory studies employing particle image velocimetry (PIV) have revealed that pile stiffness exerts a greater influence on lateral load capacity than embedment length. However, the latter becomes increasingly significant as stiffness rises (Hajialilue-Bonab et al., 2011). Consequently, accurate characterization of the soil–pile interaction under lateral loading is fundamental to achieving safe and economical design.

In typical offshore applications, monopiles exhibit low slenderness ratios, with embedded length-to-diameter (*L*/*D*) ratios ranging from 3 to 6, resulting in relatively rigid behavior (Jindal et al., 2024). Their performance is strongly influenced by the characteristics of the imposed loading, such as magnitude, number of cycles, and direction, as well as by the mechanical properties of the surrounding soil (Wei et al., 2026). Under lateral loading, stresses are transmitted to the surrounding sand through horizontal displacements, consistent with Winkler-type foundation behavior (Williams et al., 2022). For rigid monopiles, the response is dominated by rotational displacements, and the accumulation of pile-head rotation under cyclic wind and wave loading is more significant than in slender piles, making it a key factor governing long-term performance (Jalbi et al., 2020).

Offshore wind turbines are subjected to a vast number of cyclic loading events, often exceeding $10^8$ cycles over their service life (Dai et al., 2025). These repeated loadings induce cumulative displacements and rotations that must remain within strict serviceability thresholds. Monopile design is typically governed by Serviceability Limit State (SLS) requirements, which limit total rotation at the pile head to less than 1 degree, including installation tolerances (Doherty & Gavin, 2012). Despite the critical importance of long-term serviceability, predicting the accumulation of lateral displacement and rotation under realistic cyclic loading conditions remains one of the most challenging aspects of monopile design.

Although the PISA (Pile Soil Analysis) model has been developed as the state-of-the-art framework for modelling monopile behaviour in the recent years (Burd et al., 2020), the *p*–*y* curve approach, widely implemented in commercial design tools such as LPILE, has traditionally been used to estimate the lateral response of piles (Stacul et al., 2017). Nevertheless, the cyclic *p*–*y* curves adopted in many current design guidelines are primarily derived from field and laboratory tests involving fewer than 200 load cycles (Jindal et al., 2024). Consequently, the predicted pile deformations are independent of the actual number of load cycles. They may fail to capture the progressive degradation of stiffness and strength observed under high-cycle loading conditions. This limitation introduces significant uncertainty into the long-term prediction of monopile behavior under realistic offshore loading conditions.

Several experimental studies have sought to enhance understanding of cyclic lateral behavior. (Kahribt & Abbas, 2018) demonstrated that both displacement and bending moment in single piles increase with the magnitude and number of load cycles. Subsequent research by Qin & Guo (2016) and Lalicata et al. (2020) focused on characterizing the cyclic response of monopiles supporting offshore wind turbines. These studies consistently confirmed that cyclic loading leads to progressive stiffness degradation and displacement accumulation. Recently, Richards et al. (2020) reported that the ratcheting behavior of monopiles in dry sand under complex cyclic loading is significantly affected by loading directionality, with multidirectional loading producing larger rotations than unidirectional loading under comparable amplitudes.

Despite these advances, most existing studies remain limited to low-cycle testing and are predominantly conducted in dry sand or under simplified boundary conditions. The long-term cyclic response in saturated sand, which more accurately represents offshore seabed conditions, remains insufficiently investigated. Consequently, understanding of how cyclic accumulation mechanisms evolve beyond the early cycles, particularly under one-way cyclic lateral loading representative of long-term environmental actions, remains limited.

To address these knowledge gaps, the present study investigates the long-term behavior of monopile foundations under lateral cyclic loading in saturated sand through 1g physical modelling. Two lab-scale model tests were conducted, each subjected to 10,000 cycles of one-way lateral loading to simulate extended operational conditions. The experiments aim to quantify lateral displacement accumulation, evaluate pile stiffness variation with the number of cycles, and identify the key mechanisms governing long-term deformation in saturated sandy soils. The outcomes provide valuable insights for refining serviceability-based design methodologies and enhancing the reliability of monopile foundations in offshore wind turbine applications.

## 2 MATERIALS AND METHODS

### 2.1 Scaling laws and prototype

The derivation and validation of appropriate scaling laws constitute the fundamental step in any experimental study involving physical modelling. To achieve similarity between the model and its prototype, the governing physical processes must be expressed in terms of non-dimensional parameters that preserve the problem's essential physics (Lombardi et al., 2013). However, in 1g geotechnical physical modelling, it is rarely feasible to simultaneously satisfy all dimensionless groups associated with the coupled mechanical and hydraulic phenomena (Lombardi et al., 2013). Therefore, the dominant similarity relationships are prioritized according to the primary physical process under investigation. The primary dimensionless parameter governing soil response to cyclic lateral loading is shown in Equation (1).

$$\frac{P}{GD^2} \tag{1}$$

Where $P$ is the lateral load (N), $G$ is the shear modulus (GPa), and $D$ is the monopile diameter (m). This dimensionless parameter represents both the strain field in the surrounding soil and the Cyclic Stress Ratio (CSR), so preserving it ensures that the model's stiffness degradation mechanisms replicate those in the prototype (Bhattacharya et al., 2011). Using this parameter and considering that the shear modulus G in sandy soils should be assumed to be proportional to the square root of the effective stress, $G \propto \sqrt{\sigma'}$ (Wood, 2004), appropriate scaled lateral load and bending moment was calculated based on the length scaling factor ($N$), in Table 1.

Since the permeability time scale and the dynamic loading time scale are incompatible in 1g physical models without increasing the pore fluid viscosity (Wood, 2004), pore pressure effects were inevitably neglected. So, the conducted tests can be considered in drained condition. Moreover, a reduced loading frequency was employed not only to minimize excess pore pressure generation and allow its dissipation during testing, but also to avoid approaching the resonant frequency of the pile-soil system. It is also acknowledged that 1g modelling at $N = 80$ results in significantly lower effective stress levels than in the prototype. Due to the stress-dependency of granular materials, the model sand may exhibit higher dilatancy and peak friction angles than in field conditions (Ling et al., 2024). Consequently, the results presented herein are interpreted primarily in terms of governing mechanisms and trends of long-term cyclic accumulation, rather than precise quantitative predictions of prototype displacement.

In the present study, the 5 MW reference offshore wind turbine developed by the National Renewable Energy Laboratory (NREL) was selected as the prototype. Although considered relatively small by today's standards, this turbine serves as a well-documented benchmark for research purposes. The monopile foundation, characterized by a low aspect ratio ($L/D$) of about 6, behaves primarily as a rigid body, with rotational motion dominating over flexural deformation under lateral loading (Lombardi et al., 2013). Hence, the scaling of flexural rigidity was not enforced, and the monopile was modelled using steel to maintain the same material and interface properties as the prototype. Maintaining the geometric similitude ratios, particularly $t_w/D$, ensures that tip resistance is the same in the model as in the prototype.

## 2.2 Soil and model preparation

The soil used in this study is Firoozkooh standard sand No. 161, a silica-based foundry sand widely used in geotechnical engineering laboratory investigations in Iran. The sand consists of approximately 97% quartz by weight. Extensive research has been conducted on this material in recent years (Jafarzadeh et al., 2023; Maleki et al., 2023; Rahnema & Jafarzadeh, 2024), including several studies focusing on its response under high cyclic loading conditions (Tabrizi et al., 2023). The main physical and mechanical properties of this sand are summarized in Table 2, while Figure 1 illustrates its grain size distribution curves and a representative Scanning Electron Microscopy (SEM) image.

To reproduce a natural sand deposition fabric, the test specimens were prepared using the water pluviation method within a rigid steel box measuring 1 × 1 × 1 m. As the specimens were formed by water pluviation, they were considered fully saturated, and the water height was maintained 20 mm above the soil surface to prevent evaporation at the soil surface and avoid unsaturated conditions during the test. The relative density of the prepared sand deposit was approximately 27%, indicating a very loose state. This choice is consistent with conservative modelling practices, as it represents the lower end of typical offshore sand densities. It ensures that the observed responses capture worst-case behaviour of the monopile. The prepared sand deposit served as the foundation medium for the physical model tests on a scaled offshore wind turbine monopile.

*Table 1. Specifications of the prototype and physical model of the monopile (after Bhattacharya et al., 2011).*

| Quantity | Prototype (Jung et al., 2015) | Scaling Factor (Prototype / Model) | Model |
|---|---|---|---|
| Diameter ($D$) | 6 ~ 6.5 (m) | N = 80 | 7.6 (cm) |
| Wall Thickness ($t_w$) | 6 ~ 8 (cm) | | 1 (mm) |
| Embedded Length ($L$) | 30 ~ 40 (m) | | 50 (cm) |
| Mean Head-Lateral Force ($P$) | 0.6 ~ 1.6 (MN) | $N^{2.5}$ = 57243 | 20 (N) |
| Cyclic Head-Lateral Force ($P_{cyc}$) | 0.4 ~ 0.9 (MN) | | 7.5 , 15 (N) |
| Mean Head-Bending Moment ($M$) | 25 ~ 120 (MN·m) | $N^{3.5}$ = 4579467 | 10.6 (N·m) |
| Cyclic Head-Bending Moment ($M_{cyc}$) | 15 ~ 80 (MN·m) | | 3.975 , 7.95 (N·m) |

## 2.3 Setup and testing program

As shown in Figure 2a, the lateral cyclic load was applied to the monopile head using a cable connected to a rotating mechanical system mounted on a horizontally hinged beam. The beam was initially balanced by attaching counterweights to one side, as shown in Figure 2b, ensuring that the primary load could be accurately transferred to the opposite end. The desired initial static load was then determined and applied by positioning an additional weight on the horizontal beam of the loading mechanism.

Cyclic loading amplitude variation was achieved by rotating the attached mass through a DC motor. The rotation changed the distance of the mass from the hinge axis, thereby altering the effective horizontal force transmitted to the monopile via the cable (Figure 2b). The precise location of the cable connection to the beam was determined based on the applied load ranges, and a calibrated load cell was installed in-line to continuously monitor and verify the applied dynamic load during the tests (Figure 2b). Depending on the required head-bending moment, the cable was attached to the monopile at a specific lever arm above the soil surface (Figure 2a). The dynamic load frequency was controlled by adjusting the DC motor's rotational velocity.

Four Linear Variable Differential Transformers (LVDTs), two installed horizontally and two installed vertically, were used to record the monopile head's lateral and vertical displacements, allowing the calculation of rotation and verification of accidental torsion at the monopile head (Figure 2a). Additionally, to monitor the bending response of the monopile during the tests, the model monopile was instrumented with three sets of full-bridge strain gauges spaced at 166 mm intervals along its length (Figure 2a) to verify load transfer. However, bending moment profiles are outside the scope of this paper.

Three pore pressure transducers were also placed in the sand at a 50 mm span of the monopile, at two different depths, spaced 166 mm vertically from each other and from the ground surface, for continuous monitoring of excess pore pressure generation and dissipation during cyclic loading (Figure 2a). Their data confirmed that excess pore water pressure generation remained negligible throughout the tests (< 0.03 kPa). It corresponds to a variation in effective stress of less than 1%, confirming that the loading frequency was sufficient to maintain drained conditions.

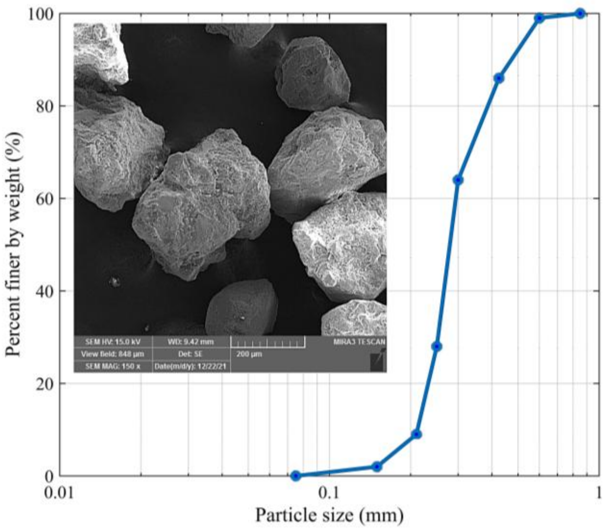


*Figure 1. Particle size distribution curve and SEM image of standard Firoozkooh sand (No. 161).*

*Table 2. Physical and mechanical properties of standard Firoozkooh sand (No. 161).*

| Parameters | $G_s$ | $e_{min}$ | $e_{max}$ | $\phi$ | $C_c$ | $C_u$ |
|---|---|---|---|---|---|---|
| **Value** | 2.65 | 0.54 | 0.94 | 33° | 1.01 | 1.39 |

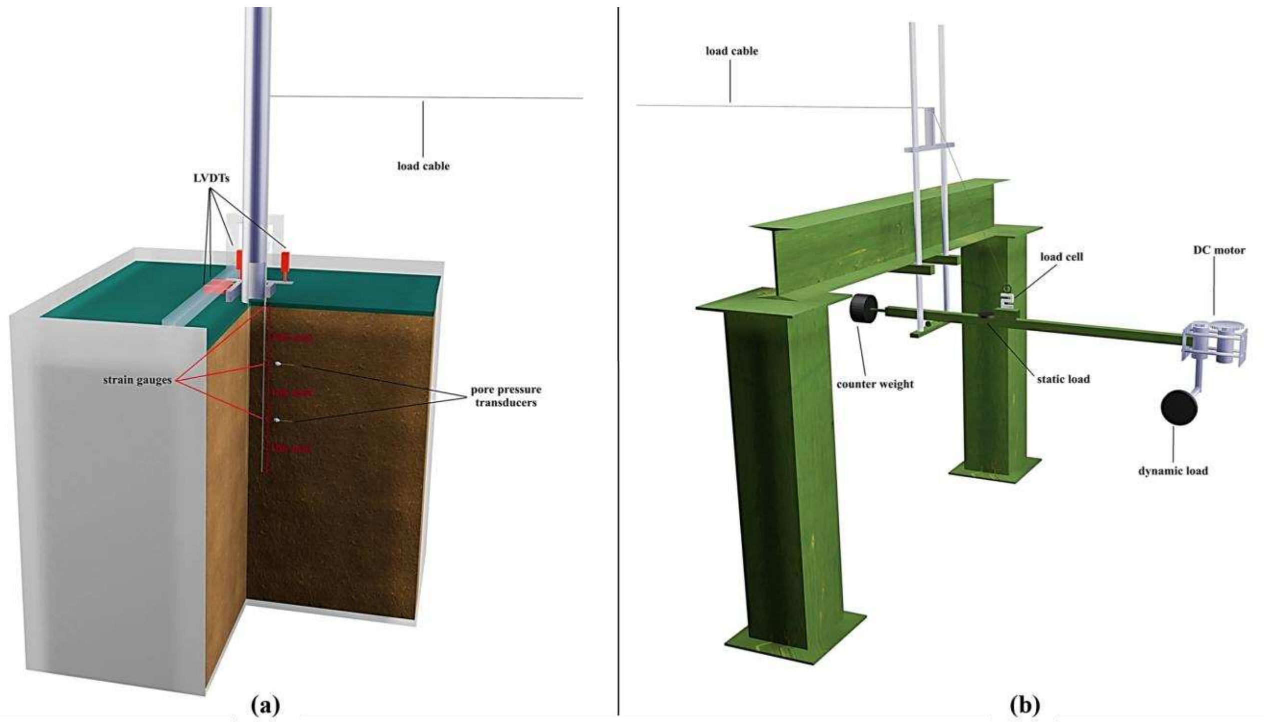


*Figure 2. Schematic view of the setup: (a) physical model setup and (b) force-controlled lateral loading mechanism.*

Three pore pressure transducers were also placed in the sand at a 50 mm span of the monopile, at two different depths, spaced 166 mm vertically from each other and from the ground surface, for continuous monitoring of excess pore pressure generation and dissipation during cyclic loading (Figure 2a). Their data confirmed that excess pore water pressure generation remained negligible throughout the tests (less than 0.03 kPa). It corresponds to a variation in effective stress of less than 1%, confirming that the loading frequency was sufficient to maintain drained conditions.

The test program includes two cyclic tests with 10,000 loading cycles at 0.33 Hz. In both tests, the average lateral force and bending moment remained constant throughout. At the same time, the dynamic lateral force and bending moment amplitudes were the variable parameters. In the second test, the dynamic lateral force amplitude was doubled, resulting in twice the dynamic bending moment, since the lever arm of the applied force is 53 cm in both cases. The sensor data are recorded with a 32-channel dynamic data logger at a sampling rate of 100 Hz to capture all changes with the highest fidelity and resolution possible.

# 3 RESULTS AND DISCUSSION

## 3.1 Accumulated lateral displacement of the monopile head

The accumulated lateral displacement at the monopile head resulting from 10,000 cycles of lateral loading is illustrated in Figure 3. As shown in Figure 3a, for the test with a lateral force amplitude of 7.5 N and a bending moment amplitude of 3.975 N·m, the rate of accumulated lateral displacement is very high during the initial cycles. However, it decreases as the number of cycles increases. For example, within the first 1,000 cycles, the accumulated displacement reaches 1.23 mm. In comparison, during the subsequent 9,000 cycles, the total additional displacement is only 0.97 mm, resulting in a final total displacement of about 2.20 mm. Ultimately, with more cycles, the accumulation rate decreases, causing the total head displacement to asymptote to a horizontal line. This trend is attributed to soil densification due to repeated loading cycles. As the number of cycles increases, the void ratio decreases, and the soil lateral stiffness increases, thereby reducing the magnitude of displacement.

A similar trend is observed in the second test; however, due to the larger lateral force and head-bending moment amplitude of 15 N and 7.95 N·m, respectively, the accumulated displacement is greater. Comparison of the two tests indicates that doubling the head-bending moment amplitude results in more than twice the accumulated displacement. The larger displacement can be attributed to the soil's nonlinear post-yielding behaviour, which results in greater displacement when larger lateral forces impose higher levels of cyclic input energy.

To better illustrate early-cycle behaviour, Figure 3b is plotted on a semi-logarithmic scale. The plot shows that during approximately the first 10 cycles, the accumulated displacement is nearly the same in both tests, suggesting that increases in cyclic head lateral force and bending moment amplitude do not significantly influence soil plastic displacement in the initial cycles. Figure 3b further indicates that the elastic lateral displacement amplitude increases with the dynamic head lateral force and the bending moment amplitude (as magnified in Figure 3b).

## 3.2 Lateral force-displacement hysteresis response

Figure 4 illustrates the hysteresis loops of lateral head displacement versus applied lateral force. Each loop corresponds to a different loading cycle and is plotted with respect to the origin to enable comparison. The results correspond to the test with a bending moment amplitude of 7.95 N·m. Because the test was conducted under force-controlled loading, the vertical size of all loops in Figure 4 is identical. The observed lateral displacement of the pile during load reversal is due to the plastic behaviour of the surrounding soil. Actually, the soil has a delayed response to lateral load reversal, and requires a finite displacement to fully mobilize the lateral resistance in the opposite direction, resulting in continued pile movement. The slope of each loop represents the soil-pile resilient stiffness. For clarity, the resilient stiffness at cycle 500 is shown in Figure 4a, and calculated using Equation (2).

$$k_R = \frac{F_{max} - F_{min}}{\Delta L_{max} - \Delta L_{min}} \quad (2)$$

Where $k_R$ is the resilient stiffness of soil (kN/m), $F_{min}$ and $F_{max}$ are the minimum and maximum applied lateral force (N) in order, and $\Delta L_{min}$ and $\Delta L_{max}$ are the minimum and maximum relative lateral displacement of the monopile head to its accumulated displacement by that cycle (mm). As shown in Figure 4a, the hysteresis loops rotate clockwise with increasing cycle number up to cycle 1500, indicating a reduction in soil resilient stiffness. It reveals that, under a constant applied force, the elastic displacement amplitude increases with each cycle. Moreover, given the drained conditions (less than 1% change in effective stress), this degradation is attributed to the accumulation of plastic volumetric strains and to the rearrangement of the loose sand fabric during the initial conditioning phase, rather than to effective stress reduction. It is associated with the high rate of displacement accumulation observed in Figure 3a (more than 60% of total displacement occurred within the first 1500 cycles).

Furthermore, the loop area, representing the energy dissipated per cycle (damping), decreases with increasing cycle number. It shows that the system dissipates more energy in the early stages of loading, which is also associated with greater plastic head displacement during the initial cycles (Figure 3a). As the cycles increase beyond 2000 (Figure 4b), the hysteresis loops rotate counterclockwise, indicating an increase in pile-soil resilient stiffness. In subsequent cycles, soil densification occurs, increasing the system's resilient stiffness and reducing the rate of displacement accumulation (Figure 3a). Between cycles 2000 and 3000, soil stiffness increases rapidly, after which the rate of increase gradually decreases. Eventually, stiffness stabilizes between cycles 8000 and 10,000. Additionally, analysis of loop areas between cycles 2000 and 10,000 shows a progressive reduction in damping, ultimately asymptote a constant value.

# 4 CONCLUSIONS

In this study, the behaviour of a monopile subjected to long-term cyclic lateral head loading was investigated through two 10,000-cycle tests with different lateral forces and the main findings are:

1) The majority of the monopile head plastic displacement occurs during early cycles and decreases as the number of cycles increases.
2) Doubling the bending moment amplitude resulted in more than double the accumulated displacement, indicating the nonlinear relationship between lateral load amplitude and accumulated displacement during cyclic loading.
3) The resilient stiffness of pile-soil system initially decreased in the first 1500 cycles, likely due to soil initial fabric degradation, but subsequently increased as soil densification developed with further cycling. Stiffness eventually stabilized between cycles 8000 and 10,000.
4) The system damping was higher during the early cycles but gradually decreased throughout the 10,000 cycles, asymptotically approaching a nearly constant level at the end.

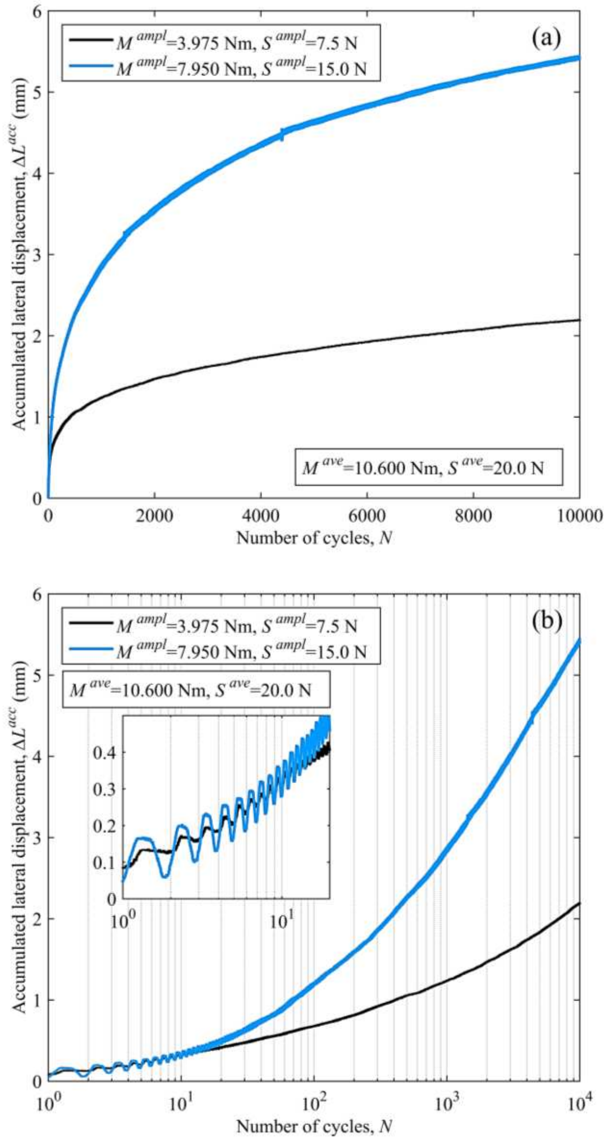


*Figure 3. Accumulation of lateral monopile head displacement during 10,000 cycles: (a) number of cycles on a linear scale; (b) number of cycles on a semi-logarithmic scale.*

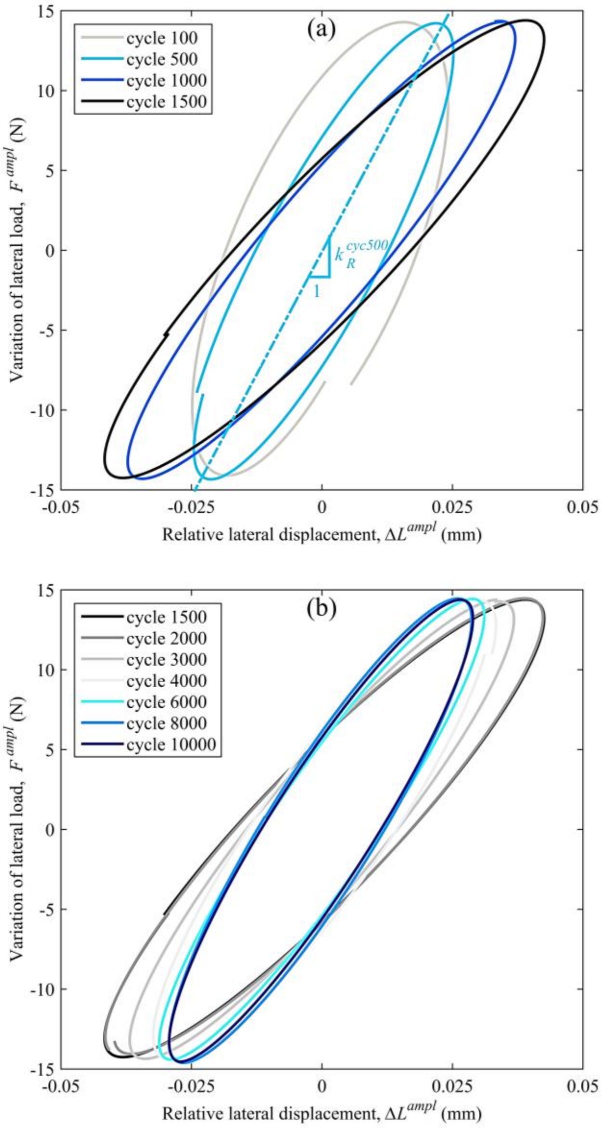


*Figure 4. Hysteresis loops of relative lateral head displacement versus applied lateral force: (a) cycles 1 to 1,500; (b) cycles 1,500 to 10,000.*

## REFERENCES


Alsharedah, Y. A. (2025). Lateral Performance of Monopile Foundations for Offshore Wind Turbines in Clay Soils: A Finite Element Investigation. *Journal of Marine Science and Engineering*, *13*(7). https://doi.org/10.3390/jmse13071222

Arvan, P. A., Raju, R. D., & Arockiasamy, M. (2023). Offshore wind turbine monopile foundation systems in multilayered soil strata under aerodynamic and hydrodynamic loads: State-of-the-art review. *Practice Periodical on Structural Design and Construction*, *28*(3), 03123001. https://doi.org/10.1061/PPSCFX.SCENG-1198

Bhattacharya, S., Lombardi, D., & Muir Wood, D. (2011). Similitude relationships for physical modelling of monopile-supported offshore wind turbines. *International Journal of Physical Modelling in Geotechnics*, *11*(2), 58-68. https://doi.org/10.1680/ijpmg.2011.11.2.58

Burd, H. J., Taborda, D. M. G., Zdravkovic, L., Abadie, C. N., Byrne, B. W., Houlsby, G. T., Gavin, K. G., Igoe, D. J. P., Jardine, R. J., Martin, C. M., McAdam, R. A., Pedro, A. M. G., & Potts, D. M. (2020). PISA design model for monopiles for offshore wind turbines: Application to a marine sand. *Geotechnique*, *70*(11). https://doi.org/10.1680/jgeot.18.P.277

Dai, S., Sweetman, B., & Tang, S. (2025). Impact of Non-Gaussian Winds on Blade Loading and Fatigue of Floating Offshore Wind Turbines. *Journal of Marine Science and Engineering*, *13*(9), 1686. https://doi.org/10.3390/jmse13091686

Doherty, P., & Gavin, K. (2012). Laterally loaded monopile design for offshore wind farms. *Proceedings of the institution of civil engineers-energy*, *165*(1), 7-17. https://doi.org/10.1680/ener.11.00003

Guo, W. D. (2006). On limiting force profile, slip depth and response of lateral piles. *Computers and Geotechnics*, *33*(1), 47-67. https://doi.org/10.1016/j.compgeo.2006.02.001

Hajialilue-Bonab, M., Azarnya-Shahgoli, H., & Sojoudi, Y. (2011). Soil deformation pattern around laterally loaded piles. *International Journal of physical modelling in geotechnics*, *11*(3), 116-125. https://doi.org/10.1680/ijpmg.2011.11.3.116

Jafarzadeh, F., Afzal, S., & Rahnema, S. (2023). مدلسازی فیزیکی رفتار شمع حرارتی منفرد در خاک خشک , Physical modeling of the behavior of a single geothermal energy pile in dry soil (in Persian). In *The 5th National Geotechnical Conference and the 2nd International Conference on Earthquake Engineering and Seismic Geotechnics*. https://en.civilica.com/doc/2061406

Jalbi, S., Hilton, J., & Jacques, L. (2020). Assessment of practical methods to predict accumulated rotations of monopile-supported offshore wind turbines in cohesionless ground profiles. *Energies*, *13*(15), 3915. https://doi.org/10.3390/en13153915

Jindal, S., Rahmanli, U., Aleem, M., Cui, L., & Bhattacharya, S. (2024). Geotechnical challenges in monopile foundations and performance assessment of current design methodologies. *Ocean Engineering*, *310*, 118469. https://doi.org/10.1016/j.oceaneng.2024.118469

Jung, S., Kim, S. R., Patil, A., & Hung, L. C. (2015). Effect of monopile foundation modeling on the structural response of a 5-MW offshore wind turbine tower. *Ocean Engineering*, *109*, 479-488. https://doi.org/10.1016/j.oceaneng.2015.09.033

Kahribt, M. A., & Abbas, J. M. (2018). Lateral response of a single pile under combined axial and lateral cyclic loading in sandy soil. *Civil Engineering Journal*, *4*(9), 1996-2010. https://doi.org/10.28991/cej-03091133

Lalicata, L. M., Rotisciani, G. M., Desideri, A., Casini, F., & Thorel, L. (2020, October). Physical modelling of piles under lateral loading in unsaturated soils. In *E3S Web of conferences* (Vol. 195, No. 01021). EDP Open. https://doi.org/10.1051/e3sconf/202019501021

Ling, D., Hu, T., Wang, J., Wang, X., Shi, C., & Tang, Y. (2024). Numerical study on the shear strength of granular materials under the low confining pressure. *Soils and Foundations*, *64*(3), 101447. https://doi.org/10.1016/j.sandf.2024.101447

Lombardi, D., Bhattacharya, S., & Wood, D. M. (2013). Dynamic soil–structure interaction of monopile supported wind turbines in cohesive soil. *Soil dynamics and earthquake engineering*, *49*, 165-180. https://doi.org/10.1016/j.soildyn.2013.01.015

Maleki Tabrizi, E., Dibazar, A. A., Hajialilue-Bonab, M., Esmatkhah Irani, A., & Assadi-Langroudi, A. (2023). The Partially Drained Behaviour of Dense Fibre-Reinforced Sands. *Sustainability*, *15*(23), 16286. https://doi.org/10.3390/su152316286

Malekjafarian, A., Jalilvand, S., Doherty, P., & Igoe, D. (2021). Foundation damping for monopile supported offshore wind turbines: A review. *Marine Structures*, *77*, 102937. https://doi.org/10.1016/j.marstruc.2021.102937

Qin, H., & Guo, W. D. (2016). Response of static and cyclic laterally loaded rigid piles in sand. *Marine Georesources & Geotechnology*, *34*(2), 138-153. https://doi.org/10.1080/1064119X.2014.979961

Rahnema, S., & Jafarzadeh, F. (2024). بررسی تاثیر دمای شمع حرارتی بر روی ظرفیت باربری نهایی آن با استفاده از مدل فیزیکی 1g, Evaluation of the effect of geothermal energy pile temperature on its ultimate bearing capacity using a 1g physical modelling (in Persian). In *11th International Conference on Modern Studies in Civil Engineering, Architecture, Urban Planning and Environment in the 21st Century*. https://en.civilica.com/doc/2060479

Richards, I. A., Byrne, B. W., & Houlsby, G. T. (2020). Monopile rotation under complex cyclic lateral loading in sand. *Géotechnique*, *70*(10), 916-930. https://doi.org/10.1680/jgeot.18.P.302

Stacul, S., Squeglia, N., & Morelli, F. (2017). Laterally loaded single pile response considering the influence of suction and non-linear behaviour of reinforced concrete sections. *Applied Sciences*, *7*(12), 1310. https://doi.org/10.3390/app7121310

Tabrizi, E. M., Tohidvand, H. R., Hajialilue-Bonab, M., Mousavi, E., & Ghassemi, S. (2023). An investigation on the strain accumulation of the lightly EICP-cemented sands under cyclic traffic loads. *Journal of Road Engineering*, *3*(2), 203-217. https://doi.org/10.1016/j.jreng.2023.03.002

Wei, X., Lin, K., & Zhou, A. (2026). An integrated model for long-term dynamic performance of monopile-supported wind turbines under operational loads with consideration of soil-structure interaction and soil property evolution. *Ocean Engineering*, *343*, 123444. https://doi.org/10.1016/j.oceaneng.2025.123444

Williams, S. A., Pelecanos, L., & Darby, A. P. (2022). A Winkler model of monopile ratcheting under long-term dynamic cyclic loading. *Ocean Engineering*, *266*, 112625. https://doi.org/10.1016/j.oceaneng.2022.112625

Wojtaszek, H., Borowski, P. F., Handschke, M., Miciuła, I., Stecyk, A., Bielawa, A., ... & Czepło, F. (2025). Wind Energy in Transition: Development, Socio-Economic Impacts, and Policy Challenges in Europe. *Energies*, *18*(11), 2811. https://doi.org/10.3390/en18112811

Wood, D. M. (2004). *Geotechnical modelling*. CRC press.